Absorption-spectral-shape analysis of the band-edge exciton in a BiI$_3$ crystal based on the exciton-phonon interaction

K. Watanabe

Department of Physics, Faculty of Liberal Arts and Education, Yamanashi University, Takeda, Kofu 400, Japan

S. Takeyama and N. Miura

Institute for Solid State Physics, University of Tokyo, Minato-ku, Tokyo 106, Japan

T. Komatsu

Department of Physics, Faculty of Science, Osaka City University, Sumiyoshi-ku, Osaka 558, Japan

(Received 16 November 1990)

We have observed optical-absorption spectra of the band-edge direct-exciton absorption line at temperatures from 4.2 to 293 K in BiI$_3$ thin-film single crystals grown by the hot-wall crystal-growth technique. The absorption spectral shape has been calculated by use of the weak-coupling exciton-phonon interaction theory. At low temperatures, the calculated results are in good agreement with the experimental measurements in the spectral regions of both the indirect-exciton edge and the direct-exciton peak.

BiI$_3$ is one of the layered semiconductors, and has attracted much attention as a material for nonlinear optics. The exciton absorption edge of the crystal is an allowed indirect type,[1] and has been relatively well investigated.[2-4] At the low-energy side of the indirect-exciton edge, several sharp absorption lines have been observed. It has been proposed that the origins of these lines are the exciton transitions localized at various stacking disorders contained in the crystal. Strong nonlinear-optical effects have been found in some of these lines.[5-7]

A direct-exciton absorption line is situated at energy a little higher than the indirect-exciton edge.[8] The Bohr radius of the direct exciton has been estimated to be very small compared with usual semiconductors.[9] In these circumstances, it is expected that the direct exciton has large optical nonlinearity and provides a typical example of exciton systems having small radii. There are, however, few investigations on the dynamical behavior of the direct exciton due to the following reason.

The absorption coefficient is very large, of the order of 8×10^5 cm^{-1} at the peak energy.[8] Therefore it has been difficult to obtain the absorption spectra of the direct exciton by transmission measurements. Accordingly, the direct-exciton absorption spectra have been obtained only by a Kramers-Kronig (KK) transformation of the reflection spectra or by transmission measurements in thin samples cleaved by an adhesive tape,[8,9] using bulk crystals.

Recently, BiI$_3$ thin-film single crystals have been grown by the hot-wall crystal-growth technique.[10,11] This has enabled us to directly observe the transmission spectra in the energy region of the direct exciton. The surface-exciton transition was clearly observed in the film crystals,[12] suggesting the good quality of the film surface.

In this paper, we present experimental results of the direct-exciton absorption spectra in a wide temperature range, and the Raman spectra of BiI$_3$ thin-film single crystals. The absorption spectral shape including both the direct-exciton peak and the indirect-exciton edge is calculated, based on the exciton-phonon interaction theory. The exciton-phonon interaction is one of the most basic problems in the studies of excitons, and has been investigated from various points of view.[13] The absorption line shape of the direct-transition-type exciton and its temperature dependence have been theoretically studied.[14]

However, experimental investigations of the line shape have been left behind, especially for semiconductors. In BiI$_3$, the absorption intensity of the direct-exciton peak is much larger than that of the band-to-band transition, and the peak persists even at room temperature. Accordingly, we can analyze the line shape of the direct exciton in a wide temperature range. BiI$_3$ is therefore one of the most suitable systems to investigate the exciton-phonon interaction.

Thin films of BiI$_3$ were grown on substrates of PbI$_2$ and CdI$_2$ single crystals by the hot-wall technique.[10,11] The surfaces of the substrates are parallel to the layer plane and perpendicular to the c axis. The direct-exciton energy of BiI$_3$ is located in the optically-transparent region of the substrates. The good crystallization of the films was confirmed by both transmission electron-diffraction measurements[11] and the absorption spectra of the direct exciton.[10]

In the optical measurements, the samples were immersed in a liquid- or gaseous-helium bath. The sample temperature was measured by a calibrated AuFe-Cr thermocouple located in the vicinity of the samples. Absorption spectra were measured for E$\perp c$ with nonpolarized light with a single-grating monochromator (Narumi RM-L21), where E is the electric-field vector of the incident light. The spectral resolution was better than 3 Å in the absorption spectra. In the measurement of the Raman spectra, the samples were excited by a tunable dye laser (Lexel model 700L) and an argon-ion laser (Lexel model 95) system. The spectra were measured for E$\perp c$ with nonpolarized light in the back-scattering configur-

ation by a double-grating monochromator (Jobin Yvon U-1000). The spectral resolution was about 0.3 Å in the Raman spectra.

A Raman spectrum of a BiI_3 thin-film crystal on a PbI_2 substrate is shown in Fig. 1. The thickness of the film was estimated to be about 100 Å. The excitation energy in the Raman spectrum was close to the direct-exciton energy. In the Raman measurements, we chose samples which had absorption intensities at the direct-exciton-peak energy that were relatively small in order to reduce the reabsorption of the scattering light. Five Raman lines were resolved in the spectrum. These lines are denoted as R_1, R_2, R_3, R_4, and R_5 in the figure, and the Raman shifts of the lines were 23, 58, 87, 97, and 113 cm^{-1}, respectively. Karasawa et al.[15] reported that the Raman shift of the most prominent lines in BiI_3 bulk crystals were 22.8, 58.5, and 113.3 cm^{-1} at 4.2 K. These lines have been assigned to the three A_g-mode optical phonons at the Γ point, which are called A, B, and C phonons, respectively. The Raman shift of R_1, R_2, and R_5 are equal to the respective energies of the A, B, and C phonons at the Γ point, while the Raman shifts of the R_3 and R_4 lines are equal to those reported for PbI_2 crystals.[16,17] The R_3 and R_4 lines result from Raman lines from the PbI_2 substrate.

The Raman intensities of R_1, R_2, and R_5 are strongly dependent on the excitation photon energy, while those of R_3 and R_4 do not change with energy. The intensities of R_1, R_2, and R_5 take the maximum around the excitation photon energy corresponding to the peak position of the direct-exciton absorption line. This fact suggests that the direct-exciton state, which is excited by the incident photon, becomes the intermediate state in the resonant Raman-scattering process. The intensity of the C-phonon Raman line was the largest among the three lines. Hence, the coupling of the C phonon with the direct exciton is expected to be the largest among the related optical phonons.

Figure 2 shows the absorption spectra of the direct exciton in a BiI_3 thin-film crystal on a PbI_2 substrate at different temperatures between 4.2 and 227 K. The thickness of the film was estimated to be 320 Å. The peak energy position and the full width at half maximum (FWHM) of the line were found to be 2.07 eV and 33 meV at 4.2 K. These values coincide with those of the bulk single crystals determined by the KK transforma-
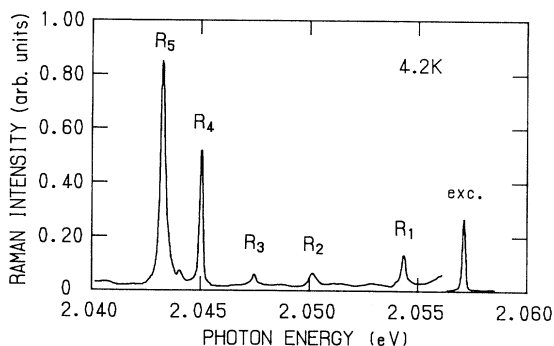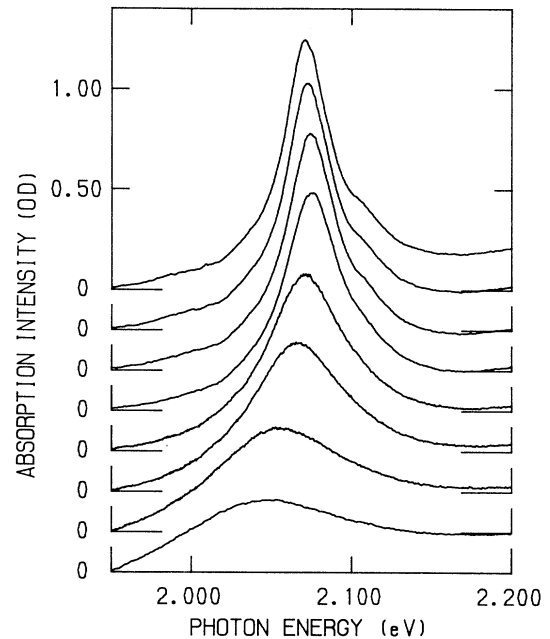

FIG. 2. Absorption spectra of a BiI_3 thin-film crystal on a PbI_2 substrate at different temperatures. OD represents optical density. Temperatures are 4.2, 23, 40, 59, 89, 121, 176, and 227 K for the spectra from the top to the bottom, respectively.

tion.[6] As the temperature is increased from 4.2 to around 50 K, the peak position shifts to the higher-energy side, while between 50 and 293 K, it shifts to the lower-energy side. At all temperatures, the line shape is Lorentzian-like, and has a tail in the higher-energy side, which is more prominent at high temperatures. Below 40 K, the FWHM is nearly constant, and above, it increases with temperature. This may be mainly due to the C phonon with a population that starts to increase from around 40 K.

Next, we discuss the width of the present exciton-absorption line. If the exciton band has its bottom at $K = 0$ and only intraband scattering is taken into account, the width of the zero-phonon line resulting from phonon scattering should become zero at $T = 0$ (K is the wave vector of the exciton, T is temperature). Consequently, the width at $T = 0$ should be determined by the inhomogeneous broadening or homogeneous broadening due to the scattering by imperfections (defects or impurities). In the case that the width is dominated by the inhomogeneous broadening, the line shape should be a Gaussian type, but the present line shape is a Lorentzian type.

For the weak-coupling exciton-phonon interaction case, the direct-transition-type exciton line has a Lorentzian shape,[14] and the width is mainly determined by the scattering probability of the $K \sim 0$ exciton which is directly created by a photon. Imperfections take part in the scattering as well as phonons. However, the origin of the large FWHM at 4.2 K (~ 30 meV) cannot be attributed to the scattering by imperfections, since the FWHM is nearly constant among the high-quality samples with different crystal-growth conditions.

We propose a speculation based on the exciton-phonon

FIG. 1. Raman spectrum of a BiI_3 thin-film crystal on a PbI_2 substrate at 4.2 K. "exc." denotes the excitation energy.

interaction to interpret the present spectral shape including the large width of the direct exciton in BiI_3 at very low temperatures. It is believed that the band-edge exciton dispersion of the K_Z direction of BiI_3 has a maximum (2.072 eV) at $K = 0$ and a minimum (2.008 eV) at the zone edge[18] (K_Z is the component parallel to the Γ-Z direction in the Brillouin zone). In such a case, the exciton at $K \sim 0$ is scattered to lower-energy states at $T = 0$ in the band, with accompanying phonon emissions, in addition to the scattering by imperfections.

We take into account the phonon side bands accurately to interpret the whole spectral shape including the indirect-exciton absorption edge. Absorption intensity $\alpha(E)$ is calculated by the following equation:

$$\alpha(E) = A_0 \frac{\Gamma(E)}{[\hbar\Gamma(E)]^2 + [E - E_{ex}(0)]^2} ,$$

where $\Gamma(E)$ is scattering probability, $E_{ex}(K)$ is the exciton energy, and A_0 is a constant. $\Gamma(E)$ was calculated for the present case by the following equations:

$$\Gamma(E) = \frac{2\pi}{\hbar} \sum_\mu \sum_i \sum_K |\beta_{\mu,i}(K)|^2 \{n[\hbar\omega_{\mu,i}(\mp K)] + \tfrac{1}{2} \pm \tfrac{1}{2}\}$$

$$\times \delta[E - E_{ex}(K) \mp \hbar\omega_{\mu,i}(\mp K)] ,$$

$$\mu = ac, op, \quad i = A \ (\mu = ac), \quad i = A, B, C \ (\mu = op)$$

$$E_{ex}(K) = \hbar^2 K_{XY}^2/(2M_{XY}) + 2J_Z\cos(a_Z K_Z) + E_0 ,$$

$$\hbar\omega_{ac,i}(k) = \hbar\omega_i(Z)\sin(a_Z k/2) ,$$

$$\hbar\omega_{op,i}(k) = \tfrac{1}{2}[\hbar\omega_i(\Gamma) + \hbar\omega_i(Z)]$$

$$+ \tfrac{1}{2}[\hbar\omega_i(\Gamma) - \hbar\omega_i(Z)]\cos(a_Z k) ,$$

where n is the phonon-population number, $\hbar\omega_{\mu,i}$ is phonon energy, M_{XY} is the exciton mass in the K_{XY} direction, $4J_Z$ is the exciton band width in the K_Z direction, E_0 is a constant, a_Z is the lattice constant in the Z direction, k is the wave vector, $\hbar\omega_i(\Gamma)$ and $\hbar\omega_i(Z)$ are the optical-phonon energies at the Γ point and the Z point,[15] respectively. The ac and op denote acoustic and optical phonons, respectively. The A, B, and C are the notations of phonon modes in BiI_3. We take into account only the intraband scattering in the lowest exciton band, and assume the deformation potential for acoustic phonons and Fröhlich electron-phonon interaction for optical phonons. The effective charge of the $1s$ exciton is assumed as follows:

$$\beta_{ac}(w) = \left[\frac{2\hbar}{9NMu}w\right]^{1/2}[-q_h(w)C_v + q_e(w)C_c] ,$$

$$\beta_{op}(w) = \left[\frac{2\pi\hbar\omega e^2}{Nv_0}\left[\frac{1}{\kappa_0} - \frac{1}{\kappa}\right]\right]^{1/2}\frac{1}{w}[-q_h(w) + q_e(w)] ,$$

$$q_i(w) = \left[1 + \left(\frac{p_i w}{2a}\right)^2\right]^{-2} , \quad i = e, h .$$

The notations in the above equations are after Toyozawa.[14] The $E_{ex}(0)$ is a constant in the present calculation. The calculated curve of $\hbar\Gamma(E)$ is shown in Fig. 3. Experimental and calculated spectra at 4.2 K near the
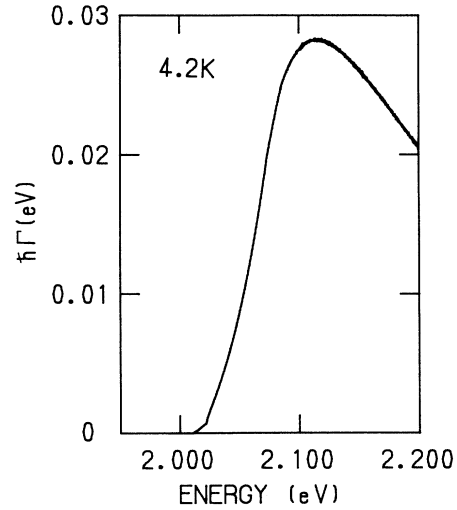

FIG. 3. Calculated $\hbar\Gamma$ at 4.2 K.

indirect-exciton edge are shown in Figs. 4(a) and 4(b). The A_e, B_e, and C_e indicate the thresholds of the indirect-exciton transitions accompanying the A-, B-, and C-phonon emissions, respectively. These structures have been assigned to the transition to the indirect-exciton state around the exciton band bottom at the zone edge.[1] The calculated and experimental curves are in good agreement. The line shape around the absorption edge is mainly determined by the density of states of the band-edge exciton.

Figure 5 shows the calculated spectra around the direct-exciton peak at different temperatures. At low temperatures, the calculated and experimental spectra agree. According to the present model, the large value of FWHM at 4.2 K of the direct-exciton line originates from the exciton intraband scattering to the lower-energy states, reflecting the characteristic feature of the present exciton band structure. Near $K = 0$, the excitons have a very short lifetime due to the scattering, and thus the excitons are relaxed to the bottom of the exciton band at the
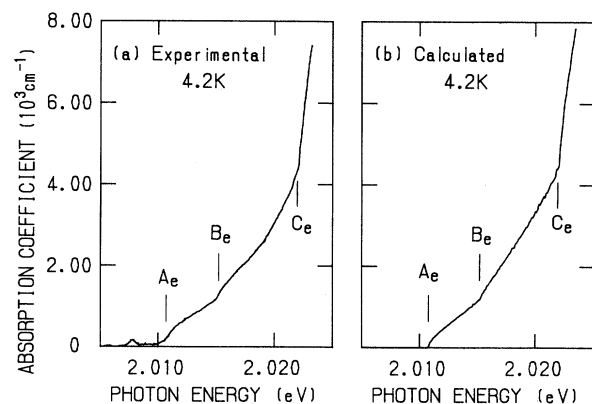

FIG. 4. (a) Absorption spectrum around the indirect-exciton absorption edge at 4.2 K. This spectrum was obtained using a BiI_3 bulk crystal. (b) Calculated spectrum around the edge at 4.2 K.
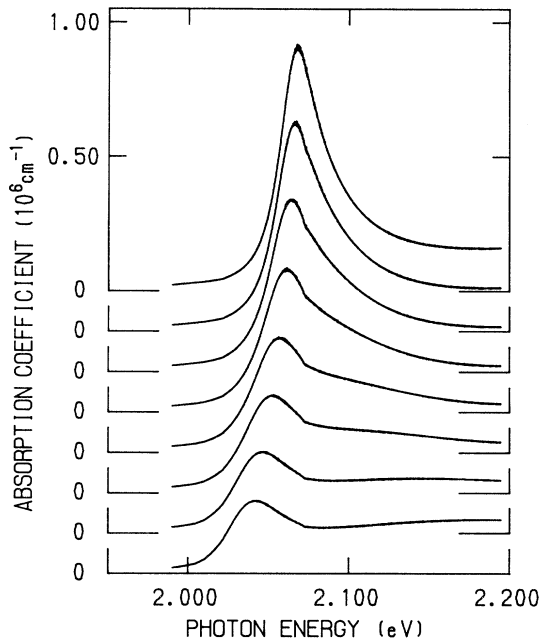
FIG. 5. Calculated spectra around the direct-exciton peak. Temperatures are 4.2, 23, 40, 59, 89, 121, 176, and 227 K for the spectra from the top to the bottom, respectively. A base line is added to each spectrum.

zone edge. In fact, the zero-phonon luminescence has not been observed at the direct-exciton energy, while the luminescences from the indirect-exciton state near the band bottom appear, being assisted by the phonon emissions.[3] This is consistent with the present model.

At high temperatures, there is a discrepancy between the calculated lower-energy tail and the experimental spectra. In BiI_3 bulk crystals, the lower-energy tail of the exciton transition obeys the Urbach rule above 77 K.[4] Hence, the discrepancy is probably due to the contribution of multiple-phonon scattering.

In conclusion, BiI_3 thin-film single crystals have been grown by the hot-wall technique. The observed Raman shifts of the films were in agreement with those of bulk crystals, indicating the high quality of the present samples. The present thin-film crystal-growth technique enabled observation of the transmission spectra of the band-edge direct exciton. The line shape of the direct exciton was analyzed in BiI_3 in a wide temperature range. So far, there have been few studies where the exciton line shape was analyzed even at room temperature among other semiconductors. The present work has become possible due to the unique characters of the direct exciton in BiI_3; namely, the large binding energy and the strong absorption intensity of the exciton transition compared with the band-to-band transitions. The calculated result is in good agreement with the observed spectral shape in the energy region from the indirect-exciton absorption edge to the direct-exciton peak at low temperatures. The exciton-phonon interaction in the weak-coupling case is considered to be applicable to the present case at low temperatures.

[1]Y. Kaifu and T. Komatsu, J. Phys. Soc. Jpn. **40**, 1377 (1976).

[2]T. Iida, M. Sakai, T. Karasawa, T. Komatsu, and Y. Kaifu, J. Phys. C **16**, 4719 (1983).

[3]T. Karasawa, T. Iida, M. Sakai, T. Komatsu, and Y. Kaifu, J. Phys. C **18**, 4043 (1985).

[4]S. Takeyama, K. Watanabe, N. Miura, T. Komatsu, K. Koike, and Y. Kaifu, Phys. Rev. B **41**, 4513 (1990).

[5]S. Tatsumi, T. Karasawa, T. Komatsu, and Y. Kaifu, Solid State Commun. **54**, 587 (1985).

[6]K. Watanabe, T. Karasawa, T. Komatsu, and Y. Kaifu, J. Phys. Soc. Jpn. **55**, 897 (1986).

[7]I. Akai, T. Karasawa, T. Komatsu, and Y. Kaifu, Phys. Status Solidi B **150**, 635 (1988).

[8]T. Komatsu and Y. Kaifu, J. Phys. Soc. Jpn. **40**, 1062 (1976).

[9]Y. Kaifu, T. Komatsu, and T. Karasawa, Sci. Rep. Tohoku Univ. Ser. 1 A **27**, Suppl. 1, 1 (1979).

[10]S. Takeyama, K. Watanabe, and T. Komatsu, Jpn. J. Appl. Phys. **29**, 710 (1990).

[11]S. Takeyama, K. Watanabe, M. Ichihara, K. Suzuki, and N. Miura, J. Appl. Phys. **68**, 2735 (1990).

[12]K. Watanabe, S. Takeyama, N. Miura, and T. Komatsu, Solid State Commun. **74**, 37 (1990).

[13]For example, M. Ueta, H. Kanzaki, K. Kobayashi, Y. Toyozawa, and E. Hanamura, in *Excitonic Processes in Solids*, edited by K. Kobayashi, Springer Series in Solid-State Vol. 60 (Springer, Tokyo, 1986).

[14]Y. Toyozawa, Prog. Theor. Phys. **20**, 53 (1958).

[15]T. Karasawa, K. Miyata, T. Komatsu, and Y. Kaifu, J. Phys. Soc. Jpn. **52**, 2592 (1983).

[16]S. Nakashima, Solid State Commun. **16**, 1059 (1975).

[17]W. M. Sears, M. L. Klein, and J. A. Morrison, Phys. Rev. B **19**, 2305 (1979).

[18]T. Karasawa, T. Komatsu, and Y. Kaifu, Solid State Commun. **44**, 323 (1982).